European Association for the Development of Renewable Energies, Environment and Power Quality

International Conference on Renewable Energies and Power Quality (ICREPQ'09)

Valencia (Spain), 15th to 17th April, 2009

Modelling and Simulation of Microturbine Generation System for on-grid and off-grid Operation Modes

Noroozian R. [1], Abedi M. [2], Gharehpetian G. B. [2] and Hosseini S. H.[3]

[1]Department of Electrical Engineering, Faculty of Engineering, University of Zanjan,
P.O.Box 45195-313, Zanjan, IRAN
E-mail: norozian@aut.ac.ir
[2]Department of Electrical Engineering, Amirkabir University of Technology,
P.O. Box 15914, Tehran, Iran, Tel: (+98) 21 6646 3504, Fax: (+98) 21 6640 6469
E-mail: abedi@aut.ac.ir, grptian@aut.ac.ir
[3]Department of Electrical and Computer Engineering, Tabriz University, Tabriz, Iran
E-mail: hosseini@tabrizu.ac.ir

Abstract. A microturbine unit (MTU) consists of a gas turbine, a permanent magnet synchronous machine (PMSM), a three phase AC-to-DC rectifier and a DC-to-AC inverter. In this paper, the detailed modelling of MTU has been developed by using PSCAD/EMTDC under different operating conditions. The mathematical model for MTU is presented. Also the suitable control strategy of DC-to-AC inverter for off-grid and on-grid condition is demonstrated, too.

Key words

Microturbine, Permanent magnet synchronous machine, Modelling and power electronic interface

1. Introduction

Microturbine unit (MTU) is well suitable for a different distributed generation applications, because the MTU is flexible in connection method, can be stacked in parallel to serve larger loads, can provide reliable power and has low-emissions profile [1]-[2]. The potential applications of the MTU configuration include peak shaving, premium power, remote power, and grid support [1]-[2]. In locations where power from the local grid is unavailable or extremely expensive to install, or the customer is far from the distribution system the MTU can be a competitive option. In this case, MTU is operated in off-grid mode. In the growing distribution system, the MTU can be a grid support. In this case, MTU is in on-grid mode. Accurate modelling is necessary to study MT units operation and impact on distribution system [2]. This paper describes the dynamic modelling of a microturbine generation system. A microturbine based DG system can generate electric power in the range of 25 to 500 kW [1-4]. They are designed so that 2 to 20 units can easily be stacked in parallel, to generate multiple of rated power [2-3]. In this paper, a model for single shaft MTU has been developed and simulated by PSCAD/EMTDC and evaluated under on-grid and off-grid operation modes.

2. MTU Configuration

Fig. 1 shows the schematic diagram of a MTU, which has been studied in this paper. The MTU components are: single-shaft turbine with its control system, high speed permanent magnet generator, power electronic interfacing (rectifier and voltage source inverter) and control system for power electronic interface. The DC bus, shown in Fig. 1, is assumed to be lossless.

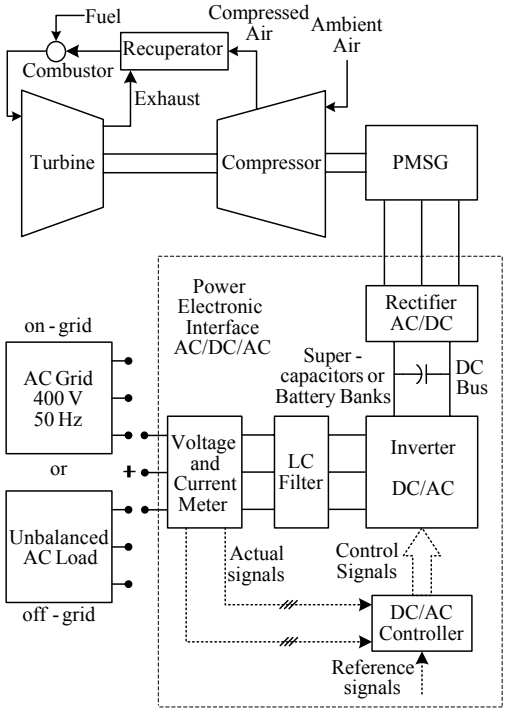

Fig. 1. Schematic diagram of MTU

Microturbine operates in the thermodynamic cycle, known as the Brayton cycle [4]-[7]. The produced rotating mechanical power in the turbine turns both compressor and generator. The high speed generator of the single shaft design is a permanent magnet synchronous generator (PMSG). This generator requires that the high frequency (about 1.6 kHz) AC output be rectified to DC for use in the DC grid, inverted back to 50 (or 60) Hz AC for use in the AC grid [4]-[8]. Power electronic interface in the single shaft microturbine is a critical component. Microturbine is generally equipped with controls that allow the unit to be operated either in parallel with, or independent of the grid.

3. Modelling of Microtubine

The block diagram of the single shaft gas turbine is shown in Fig. 2. The model includes the temperature control, fuel system, turbine dynamic, speed governor and acceleration control blocks. The output of the speed control, temperature control, and acceleration control are all inputs of a low value select (LVS) block, whose output is the input of fuel system.

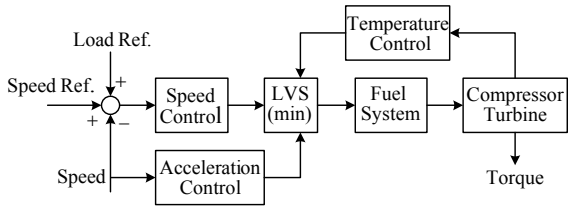

Fig. 2. Block diagram microturbine

A. Speed and Acceleration Control

Fig. 3 shows the block diagram of the speed governor control and acceleration control systems. The inputs are the load demand reference, speed reference and rotor speed of the permanent magnet generator [4].

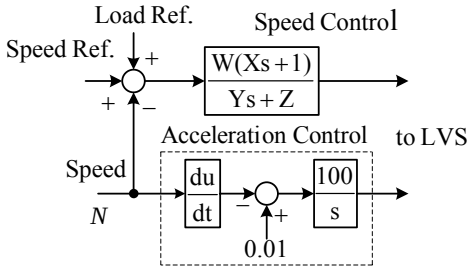

Fig. 3. Block diagram of the Speed and Acceleration control

As shown in Fig. 3, the speed governor controller has been modeled by using the lead-lag transfer function, where W is the controller gain, X (Y) is the governor lead (lag) time constant, and Z is a constant representing the governor droop or isochronous modes. Acceleration control is used during turbine startup to limit the rate of the rotor acceleration. If the operating speed of the system is close to its rated speed, the acceleration control system could be eliminated, which is the case in this study [4].

B. Fuel System

The fuel control system scheme is shown in Fig. 4. It consists of series blocks of the valve positioner and flow dynamic. The valve positioner transfer function is presented by following equation [4]-[5]:

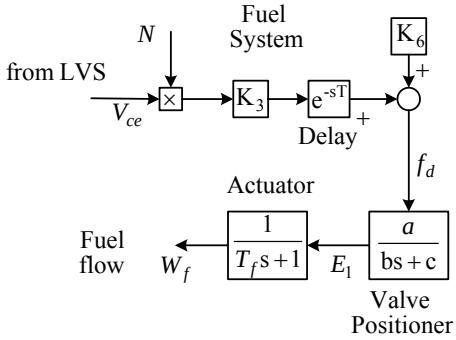

Fig.4. Block diagram of fuel system

$$E_1 = \frac{a}{bs+c} f_d \quad (1)$$

And for the flow dynamic transfer function, we have:

$$W_f = \frac{1}{T_f s+1} E_1 \quad (2)$$

Where, a is the valve positioner gain, b and T_f are the valve positioner and fuel system time constant. c is a constant. f_d and E_1 are the input and output of the valve positioner and W_f is the fuel demand signal in per unit.

C. Compressor-Turbine

Fig. 5 shows the gas turbine block diagram. The signals to the gas turbine are the fuel flow, W_f (signal from the fuel control) and the speed deviation, ΔN. The output signals are the turbine torque. The gas turbine dynamic transfer function is expressed by following equation [4]-[5]:

$$W_{f2} = \frac{1}{T_{CD}s+1} W_f \quad (3)$$

Where, T_{CD} is the gas turbine dynamic time constant. The torque characteristic of the single shaft microturbine is the function of the following equation:

$$f_2 = a_{f2} + b_{f2}.W_{f2} + c_{f2}.\Delta N \quad (4)$$

Where, f_2 is a function whose inputs are fuel flow and turbine speed.

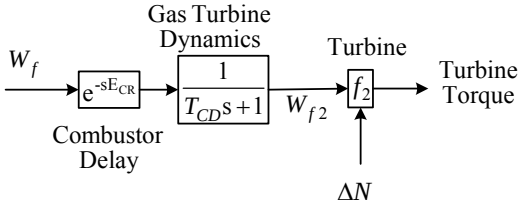

Fig. 5. Block diagram of compressor-turbine

D. Temperature Control

Fig. 6 shows the temperature controller block diagram. The input to temperature controller is the fuel flow and turbine speed and the output is temperature control signal to the LVS. The fuel burned in combustor results in turbine torque and in exhaust gas temperature. The exhaust temperature characteristic of the single shaft microturbine is the function of the following equation [4]-[5]:

$$f_1 = T_R - a_{f1}.(1 - W_{f1}) + b_{f2}.\Delta N \quad (5)$$

Where, f_1 is a function whose inputs are fuel flow and turbine speed. As shown in Fig. 6, the exhaust temperature is measured using a set of thermocouples incorporating radiation shields.

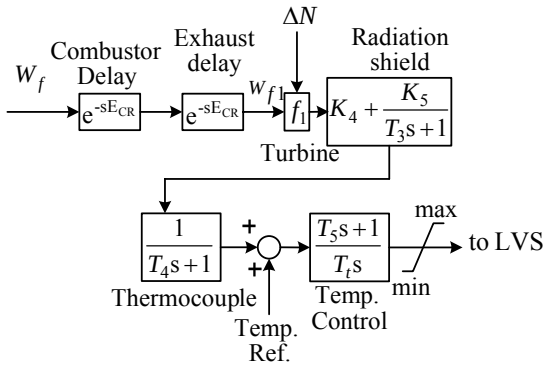

Fig. 6. Block diagram of temperature control

The output of the thermocouple is compared with a reference value. In Fig. 6, K_4 and K_5 are constant in radiation shield transfer function. T_3 and T_4 are the time constant of the radiation shield and thermocouple transfer function, respectively. T_5 and T_t are the time constant of the temperature control transfer function. When the temperature control output signal becomes lower than the speed controller output, the former value will pass through the LVS to limit the turbine's output and the turbine operates on temperature control mode.

4. Permanent Magnet Synchronous Generator Model

The electric power is produced by using high speed PSMG. The structure of high speed PSMG is presented in [8]. In this paper, the output frequency of PSMG is 1.6 kHz and the machine output power is 30 kW and terminal line-to-line voltage is 480. The equivalent circuits, considering the iron loss, are shown in Fig. 7. The following equations, expressed in the rotor reference frame (d-q frame), have has been used to model PSMG [4]-[8]:

For electrical equations, we have:

$$v_d = R_s i_d + L_d \frac{di_d}{dt} - L_q p \omega_r i_q \quad (6)$$

$$v_q = R_s i_q + L_q \frac{di_q}{dt} + L_d p \omega_r i_d + \lambda p \omega_r \quad (7)$$

$$T_e = 1.5 p[\lambda i_d + (L_q - L_d) i_d i_q] \quad (8)$$

Where,

L_d , L_q : d-axis, q-axis inductance, respectively,

R_s : Stator winding resistance,

i_d , i_q : d-axis, q-axis current, respectively,

v_d , v_q : d-axis, q-axis voltage, respectively,

ω_r : Angular velocity of rotor,

λ : Flux linkage,

P : Number of poles and

T_e : Electromagnetic torque.

For mechanical equations, we have:

$$\frac{d\omega_r}{dt} = \frac{1}{J}(T_e - T_{shaft} - F\omega_r) \quad (9)$$

$$\frac{d\theta_r}{dt} = \omega_r \quad (10)$$

Where,

J : Combined inertia of rotor and load,

T_{shaft} : Shaft mechanical torque,

F : Combined viscous friction of rotor and load and

θ_r : Rotor angular position.

5. Power Electronic Interface

Power conditioning unit consist of a rectifier-inverter system with DC link. It is a general configuration of power electronic interface in the MT units. The high frequency electric power of PSMG must be converted to DC, inverted back to 60 or 50 Hz AC and filtered to reduce harmonic distortion. An IGBT based PWM inverter is used with a 2 kHz carrier frequency. The inverter injects AC power from DC link of the MTU to the AC distribution system [9-10]. The MT units are connected in parallel to achieve the required total system capacity and provide a level of redundancy. Grid connected mode (on-grid mode) allows the MTU to operate parallel to the grid, providing base loading and peak shaving and grid support. Stand alone mode (off-grid mode) allows the MTU to operate completely isolated from the grid. In dual mode, the MTU can switch between these two modes automatically. Two different control strategies have been considered [11-12]:

- P-Q control strategy for on-grid operation mode and
- V-f control strategy for off-grid operation mode.

A. ON-GRID OPERATION

In this operation mode, the inverter must regulate the DC link voltage at 0.75 kV, and control the active and reactive powers injected into the AC grid, considering the set points, P_{ref} and Q_{ref} . These set points can be chosen by the customer or remote power management units. The P-Q control strategy is shown in Fig. 7. A phase lock loop (PLL) is used to synchronize the PWM inverter with the grid. In j) is used, resulting in a simpler

and faster control system. The reference current calculation box, in Fig. 7, calculates reference currents are as follows:

$$\begin{bmatrix} v_0 \\ v_\alpha \\ v_\beta \end{bmatrix} = \sqrt{\frac{2}{3}} \begin{bmatrix} \frac{1}{\sqrt{2}} & \frac{1}{\sqrt{2}} & \frac{1}{\sqrt{2}} \\ 1 & -\frac{1}{2} & -\frac{1}{2} \\ 0 & \frac{\sqrt{3}}{2} & -\frac{\sqrt{3}}{2} \end{bmatrix} \begin{bmatrix} v_a \\ v_b \\ v_c \end{bmatrix} \quad (11)$$

$$\begin{bmatrix} i_0 \\ i_\alpha \\ i_\beta \end{bmatrix} = \sqrt{\frac{2}{3}} \begin{bmatrix} \frac{1}{\sqrt{2}} & \frac{1}{\sqrt{2}} & \frac{1}{\sqrt{2}} \\ 1 & -\frac{1}{2} & -\frac{1}{2} \\ 0 & \frac{\sqrt{3}}{2} & -\frac{\sqrt{3}}{2} \end{bmatrix} \begin{bmatrix} i_a \\ i_b \\ i_c \end{bmatrix} \quad (12)$$

$$\begin{bmatrix} P_0 \\ P \\ Q \end{bmatrix} = \begin{bmatrix} v_0 & 0 & 0 \\ 0 & v_\alpha & v_\beta \\ 0 & -v_\beta & v_\alpha \end{bmatrix} \begin{bmatrix} i_0 \\ i_\alpha \\ i_\beta \end{bmatrix} \quad (13)$$

$$\begin{bmatrix} i_{\alpha,ref} \\ i_{\beta,ref} \end{bmatrix} = \frac{1}{v_\alpha^2 + v_\beta^2} \begin{bmatrix} v_\alpha & -v_\beta \\ v_\beta & v_\alpha \end{bmatrix} \begin{bmatrix} P_{ref} \\ Q_{ref} \end{bmatrix} \quad (14)$$

The zero-sequence current in the zero coordinate reference is i_o.

$$i_{0,ref} = i_0 \quad (15)$$

Finally, the $\alpha - \beta - 0$ inverse transformation box of Fig. 6 calculates the three-phase current references to be fed into the Hysteresis Current Control (HCC) scheme by the following equation:

$$\begin{bmatrix} i_{a,ref} \\ i_{b,ref} \\ i_{c,ref} \end{bmatrix} = \sqrt{\frac{2}{3}} \begin{bmatrix} \frac{1}{\sqrt{2}} & 1 & 0 \\ \frac{1}{\sqrt{2}} & -\frac{1}{2} & \frac{\sqrt{3}}{2} \\ \frac{1}{\sqrt{2}} & -\frac{1}{2} & -\frac{\sqrt{3}}{2} \end{bmatrix} \begin{bmatrix} i_{0,ref} \\ i_{\alpha,ref} \\ i_{\beta,ref} \end{bmatrix} \quad (16)$$

The HCC technique determines the switching pattern of the DC/AC inverter.

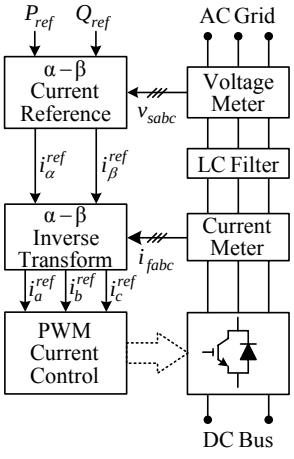

Fig. 7. P-Q control scheme

B. OFF-GRID OPERATION

In this control mode, MTU should supply AC loads, such as sensitive, nonlinear and unbalanced loads. Fig. 8 shows the control scheme, which regulates the voltage and frequency of the islanded operation mode. In the design of the V-f controller, the frequency ω is obtained by a Phase Lock Loop (PLL), which measures the AC voltage of the AC distribution network. In this case, the load voltage is regulated at desired voltage amplitude and phase by a PI controller using $a-b-c$ to $d-q-0$ and visa transformations. LC filter is used to eliminate switching harmonics.

As shown in Fig. 8, the reference voltage calculation box calculates the reference voltages. The load voltages are detected and then transformed into synchronous $d-q-0$ reference frame using equation 17:

$$\begin{bmatrix} V_{ld} \\ V_{lq} \\ V_{l0} \end{bmatrix} = T_{abc}^{dq0} \begin{bmatrix} V_{la} \\ V_{lb} \\ V_{lc} \end{bmatrix} \quad (17)$$

$$T_{abc}^{dq0} = \frac{2}{3} \begin{bmatrix} cos(\omega t) & cos(\omega t - 120^\circ) & cos(\omega t + 120^\circ) \\ -sin(\omega t) & -sin(\omega t - 120^\circ) & -sin(\omega t + 120^\circ) \\ 1/2 & 1/2 & 1/2 \end{bmatrix}$$

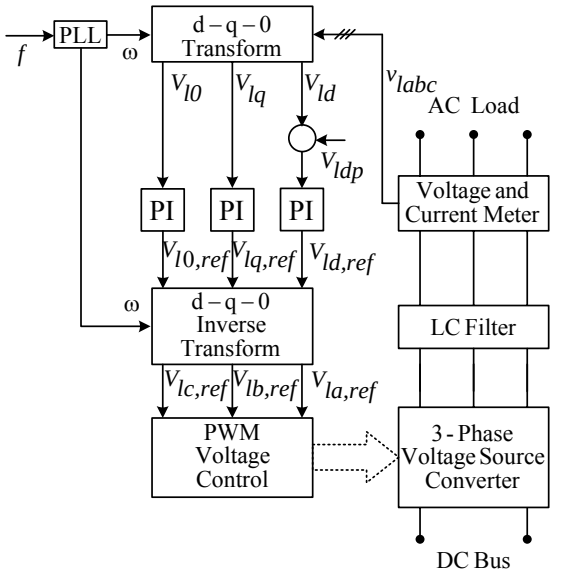

Fig. 8: V-f Control scheme

The load voltage should be sinusoidal with constant amplitude and frequency. So, the expected load voltages in $d-q-0$ reference frame have only one value, i.e. $V_{ldp} = \frac{\sqrt{2}}{\sqrt{3}} 0.4$. The reference voltage is calculated, as follows:

$$\begin{bmatrix} V_{ld}^{ref} \\ V_{lq}^{ref} \\ V_{l0}^{ref} \end{bmatrix} = \begin{bmatrix} V_{ld} \\ V_{lq} \\ V_{l0} \end{bmatrix} - \begin{bmatrix} V_{ldp} \\ 0 \\ 0 \end{bmatrix} \quad (18)$$

This means that V_{ldqo} in the equation (18) should be adjusted at the constant value V_{ldp}. V_{ldqo} voltages after

passing through a PI block are transformed into $a-b-c$ synchronous reference frame, in order to obtain the reference voltage for the PWM voltage control system.

6. Simulation Results

In this paper, the microturbine generation system units have been investigated to provide the impacts of MTU on distribution system operation. The MTU system, shown in Fig. 1, has been modeled and simulated by PSCAD/EMTDC software. The simulation parameters are given in Appendix. The simulation scenarios are focused on the on-grid and off-grid suitable operation also supplying dead load. The Simulation results are presented for different operating conditions. All time functions are in seconds. Speed reference was kept constant at 1 p.u. for all simulations.

A. ON-GRID OPERATION

In the on-grid operation mode, P-Q control scheme is applied to MTU. Fig. 9 shows active power injected to the AC grid. In this simulation, the active power reference, P_{ref} =8 kW is changed at t=10 s to 16 kW. Also, at t=20 s the active power reference, P_{ref} is decreased to 8 kW. As shown in Fig. 9, the active power injected into the AC grid matchs the above active power reference variations.

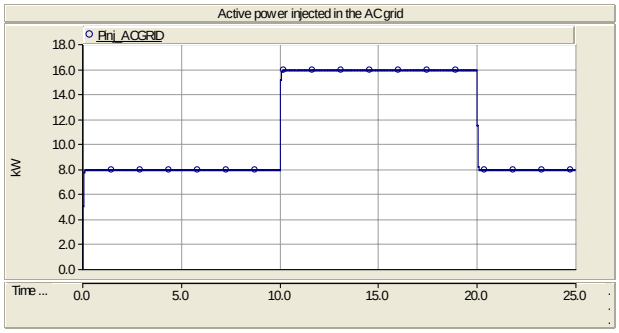

Fig. 9. Active power injected to AC grid

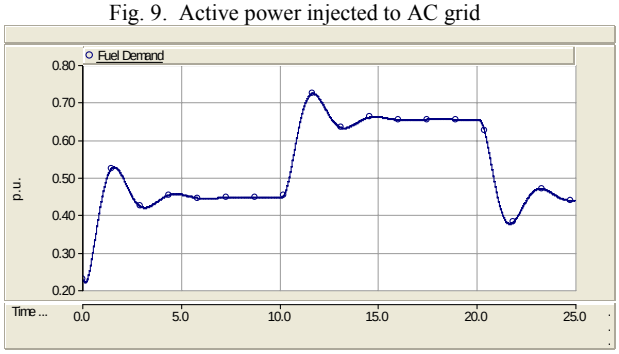

Fig. 10. Fuel demand signal of microturbine

Fuel demand signal is shown in Fig. 10. As shown in Fig. 10, fuel demand in no-load condition (t=0 s) is equal to 0.23 p.u.. The AC active power reference variation is applied at t=0 s, then the fuel demand for combustion process is increased rapidly. Also, at t=10 s, fuel demand for combustion process is decreased rapidly. Note that the fuel signal is 0.45 p.u at 8 kW and increase to 0.67 p.u. at 16 kW. The developed electromagnetic torque and the shaft torque T_{shaft} are shown in Fig. 11. The shaft torque and electromagnetic torque are equal at steady state. The electromagnetic torque is fluctuated with this variation. Figures 12 and 13 show the rotor speed and turbine mechanical output torque, which matchs the load variation requirements.

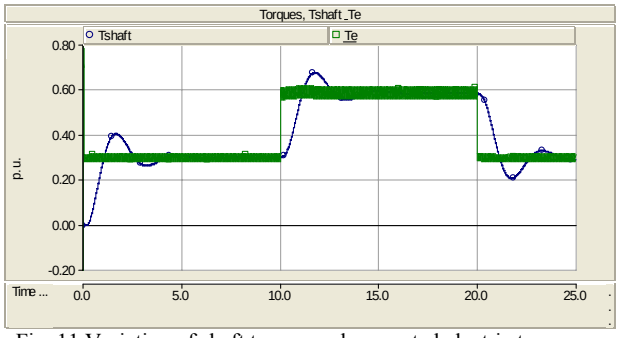

Fig. 11 Variation of shaft torque and generated electric torque

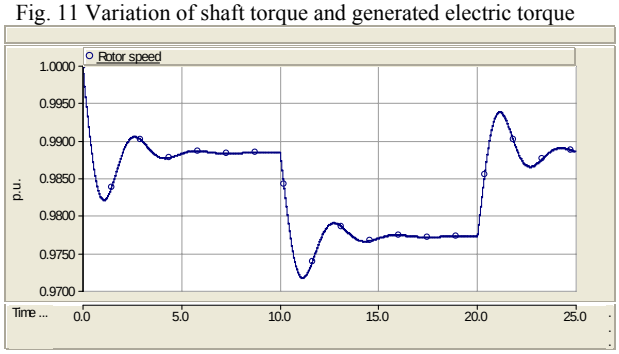

Fig. 12. Rotor speed variations

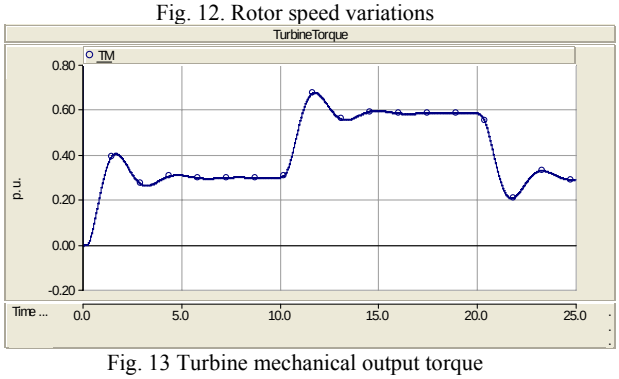

Fig. 13 Turbine mechanical output torque

As shown in Fig. 12, at t=0 s the rotor speed is equal to 1 p.u., when the MTU is connected to the AC grid. The turbine output mechanical torque (Fig. 13), with a time delay follows the variations of the active power reference.

Fig. 14 shows DC bus voltage of the uncontrolled rectifier, which matchs the grid condition. As shown in Fig. 14, when the MTU is connected to the AC grid, the DC bus voltage drops and returns to its original value. Figures 15 and 16 show the 50 Hz voltage across the AC grid and 3-phase line current. The voltage source DC-to-AC inverter maintains the sinusoidal waveform. The AC grid line current changes with active power reference variation. This verifies the effectiveness of the P-Q control strategy for the on-grid operation mode.

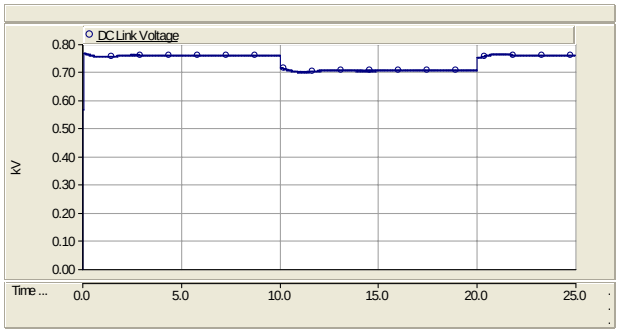

Fig. 14. DC bus voltage of the MTU system

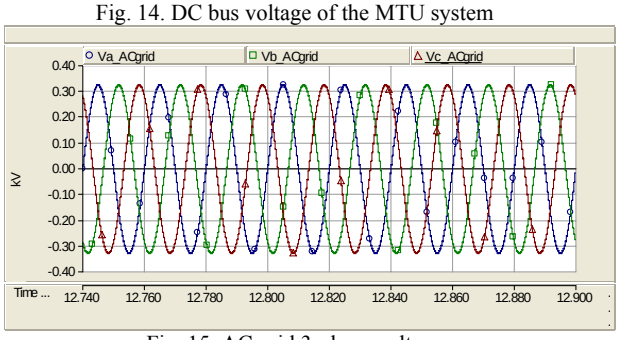

Fig. 15. AC grid 3-phase voltage

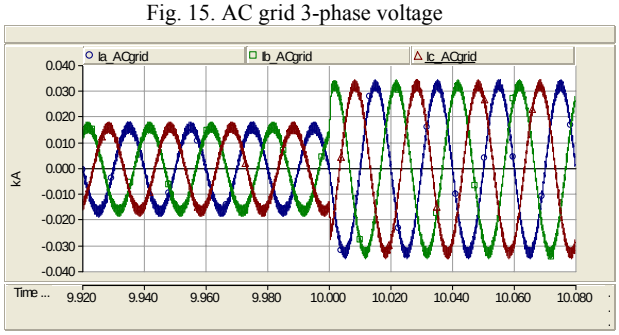

Fig. 16. AC grid line current

B. OFF-GRID OPERATION

In the off-grid operation mode, the performance of the MTU is studied by connection it to a dead load. Fig. 17 shows the active power consumed by dead loads. As shown in Fig. 17, initially the system is supplying the dead load of 16 kW. At t=10 s the load is decreased to 8 kW and then at t=20 s increased to 16 kW.

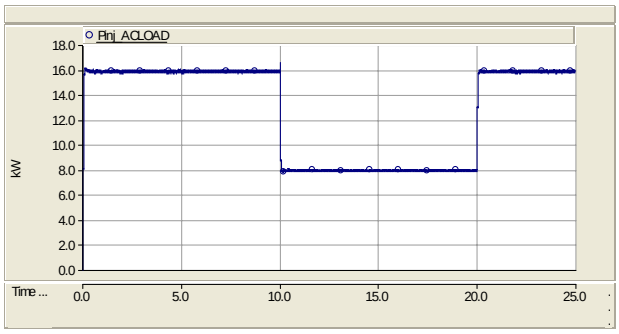

Fig. 17. Active power consumed by AC load

Fig. 18 shows the fuel consumed by the micoturbine under the load variation. As shown in Fig. 18, fuel demand in no-load condition (t=0 s) is equal to 0.23 p.u.. The load variation is applied at t=0 s, then the fuel demand for combustion process is increased rapidly. Also, at t=10 s, fuel demand for combustion process is decreased rapidly. The developed electromagnetic torque and the shaft torque T_{shaft} are shown in Fig. 19. The shaft torque and electromagnetic torque are approximately equal at steady state condition. The electromagnetic torque is fluctuated with this dead load variation. Figures 20 and 21 show the rotor speed and turbine mechanical output torque, which matchs the load variation requirements.

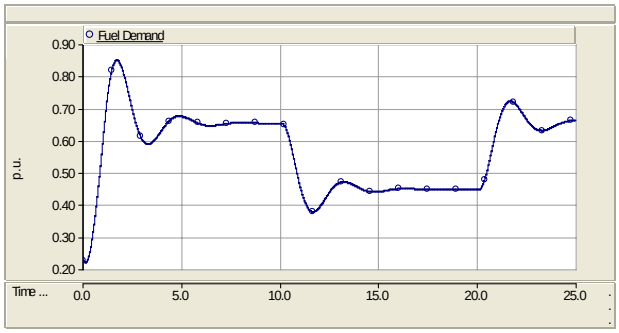

Fig. 18. Fuel demand signal of microturbine

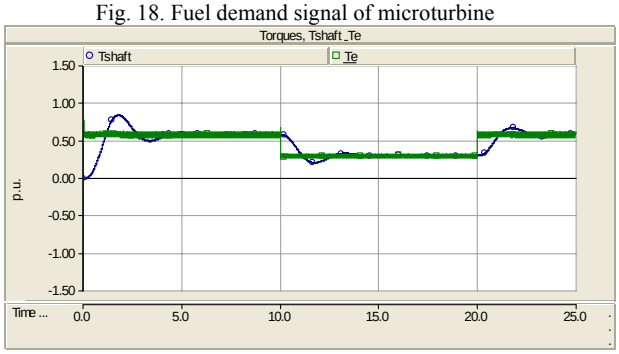

Fig. 19 Variation of shaft torque and generated electric torque

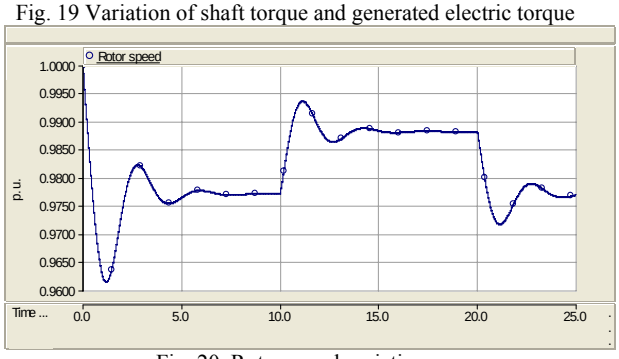

Fig. 20. Rotor speed variations

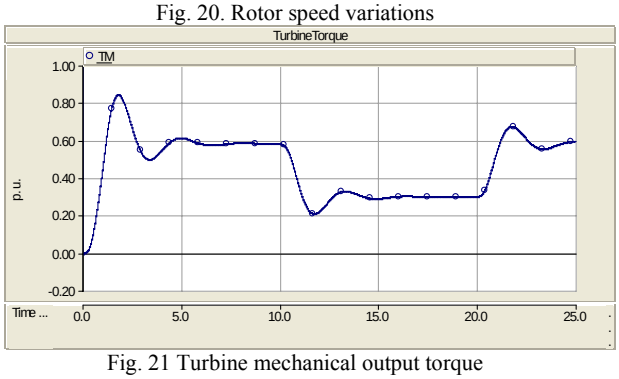

Fig. 21 Turbine mechanical output torque

Fig. 22 shows the DC bus voltage of the uncontrolled rectifier. The DC bus voltage fluctuates and returns to its

original value. Figures 23 and 24 show the 50 Hz voltage across the dead load and 3-phase line current. The voltage source DC-to-AC inverter maintains the output at the desired level. The AC voltage level across the load remains unchanged (at the reference value V_{ldp}). This point shows the ability of the voltage source DC-to-AC inverter to control its output voltage. The 3-phase line current at load terminals changes with the load variation. It should be noted that the frequency of output voltage of the PMSG is over 1.6 kHz and at the load terminals, is 50 Hz. This point verifies the effectiveness of the V-f control strategy for the off-grid operation mode.

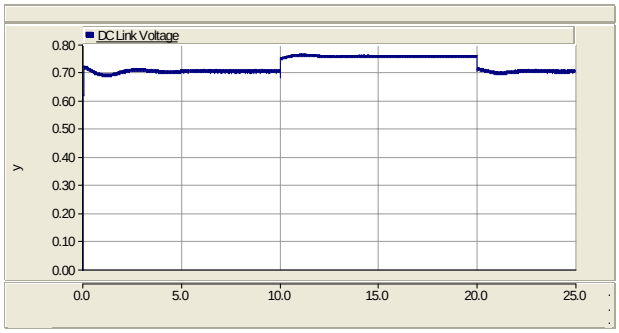

Fig. 22. DC bus voltage of MTU system

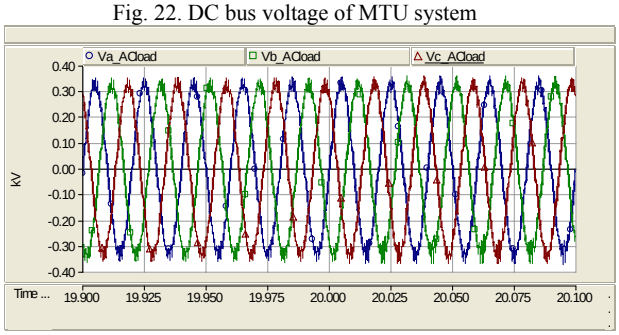

Fig. 23. Voltage at load terminals

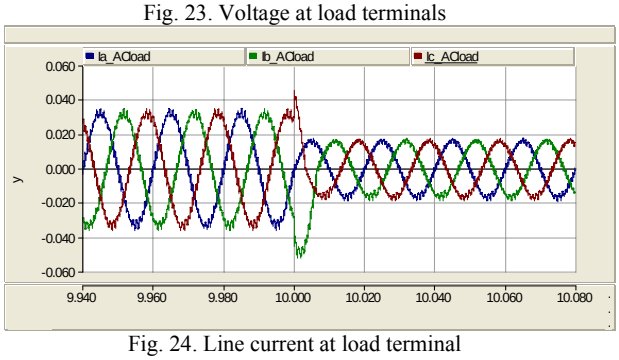

Fig. 24. Line current at load terminal

7. Conclusion

The modeling of a single-shaft MTU suitable for off-grid (isolated) and on-grid operation modes is presented in this paper. Detailed modeling of MTU with its control systems has been modeled and simulated by using PSCAD/EMTDC software. The simulation of on-grid and off-grid operation modes shows that the presented model is suitable for dynamic studies.

REFERENCES

[1] CIGRE Technical Brochure on Modeling New Forms of Generation and Storage, November 2000.

[2] Gaonkar, D.N., Patel, R.N, "Modeling and simulation of microturbine based distributed generation system," *Power India Conference, 2006 IEEE*, 10-12 April 2006.

[3] B. Yousefpour, G. Gharehpetian, R. Noroozian, M. Nafar "Simulations control of voltage and power of microturbine in distribution network," *CIRED2005, 18th international conference of electricity distribution*, Turin 6-9 June 2005.

[4] S. Guda, C. Wang, M. Nehrir, "Modeling of Microturbine Power Generation Systems, Electric Power Components and Systems," *Volume 34, Number 9, September 2006, pp. 1027-1041(15).*

[5] M. Z. C. Wanik and I. Erlich, "Dynamic Simulation of Microturbine Distributed Generators integrated with Multi-Machines Power System Network," *2nd IEEE International Conference on Power and Energy (PECon 08), December 1-3, 2008, Johor Baharu, Malaysia.*

[6] Al-Hinai, A.; Schoder, K.; Feliachi, A., "Control of grid-connected split-shaft microturbine distributed generator," *System Theory, 2003. Proceedings of the 35th Southeastern Symposium,* 16-18 March 2003 Page(s): 84 – 88.

[7] L. N. Hannett, Afzal Khan, "Combustion Turbine Dynamic Model Validation from Tests," *IEEE Transactions on Power Systems*, Vol. 8, No. 1, February 1993

[8] Ahn, J.B., Jeong, Y.H., Kang, D.H., Park, J.H, "Development of high speed PMSM for distributed generation using microturbine," Industrial Electronics Society, 2004. IECON 2004. 30th Annual Conference of IEEE, Vol. 3, 2-6 Nov. 2004 Volume: 3, on page(s): 2879- 2882.

[9] R. Lasseter, "Dynamic Models for Microturbines and Fuel Cells," IEEE PES Summer Meeting, 2001.

[10] Al-Hinai, A. Feliachi,"Dynamic Model of a Microturbine Used as a Distributed Generator," IEEE Proc. 34-th Southeastern Symposium on System Theory, 2002, pp: 209- 213.

[11] Bertani, C. Bossi, F. Fornari, S. Massucco, S. Spelta, F. Tivegna, "A microturbine generation system for grid connected and islanding operation," *Power Systems Conference and Exposition, 2004. IEEE PES*, Vol. 1, 10-13 Oct. 2004, Page(s): 360 - 365.

[12] O. Fethi, L.-A. Dessaint, K. Al-Haddad, "Modeling and simulation of the electric part of a grid connected microturbine," Power Engineering Society General Meeting, 2004. IEEE, Vol.2, 6-10 June 2004 Page(s): 2212 – 2219.